

## EARTH SCIENCES

# The frequency and extent of sub-ice phytoplankton blooms in the Arctic Ocean

Christopher Horvat,<sup>1\*</sup> David Rees Jones,<sup>2,3</sup> Sarah Iams,<sup>1</sup> David Schroeder,<sup>4</sup>  
Daniela Flocco,<sup>4</sup> Daniel Feltham<sup>4</sup>

In July 2011, the observation of a massive phytoplankton bloom underneath a sea ice–covered region of the Chukchi Sea shifted the scientific consensus that regions of the Arctic Ocean covered by sea ice were inhospitable to photosynthetic life. Although the impact of widespread phytoplankton blooms under sea ice on Arctic Ocean ecology and carbon fixation is potentially marked, the prevalence of these events in the modern Arctic and in the recent past is, to date, unknown. We investigate the timing, frequency, and evolution of these events over the past 30 years. Although sea ice strongly attenuates solar radiation, it has thinned significantly over the past 30 years. The thinner summertime Arctic sea ice is increasingly covered in melt ponds, which permit more light penetration than bare or snow-covered ice. Our model results indicate that the recent thinning of Arctic sea ice is the main cause of a marked increase in the prevalence of light conditions conducive to sub-ice blooms. We find that as little as 20 years ago, the conditions required for sub-ice blooms may have been uncommon, but their frequency has increased to the point that nearly 30% of the ice-covered Arctic Ocean in July permits sub-ice blooms. Recent climate change may have markedly altered the ecology of the Arctic Ocean.

## INTRODUCTION

Phytoplankton are a fundamental component of Earth's oceanic ecosystem and carbon cycle. These photosynthetic organisms inhabit the upper layers of the sunlit ocean, converting carbon dioxide into the organic compounds that sustain oceanic life. Through their growth and decay, they form the foundation of the oceanic food web and constitute a major sink for atmospheric CO<sub>2</sub> (1). Phytoplankton populations undergo periods of rapid growth, known as "blooms," which occur annually and semiannually in many of the world's ice-free oceans (2). In the Arctic, blooms are traditionally assumed to occur annually at the retreating sea ice edge (3). Because sea ice is optically thick, with a high albedo, regions underneath a full sea ice cover have been considered incapable of supporting photosynthetic life. This paradigm was overturned in July 2011 by the observation of a "massive" phytoplankton bloom underneath a region of the Arctic fully covered by sea ice (4), with concentrations of particulate organic carbon among the highest ever recorded in the world's oceans. During the period in which the bloom was observed, the sea ice was heavily covered by melt ponds, which form on the sea ice surface from melting snow and ice in the spring and summer. Because they have a lower albedo than bare ice, it has been hypothesized that melt ponds can transmit sufficient light through the thinner Arctic ice cover and sustain primary production, even when the ocean is fully ice-covered (5).

There has been recent speculation about the extent and frequency of phytoplankton blooms under Arctic sea ice (6). If sub-ice blooms are common, then the annual amount of primary production and carbon fixation occurring beneath the sea ice in the Arctic Ocean may have been underestimated by an order of magnitude (4, 7). Therefore, the focus of this study is to investigate the potential occurrence of these blooms in the modern Arctic and examine the changing potential for

these blooms over the past 30 years, leveraging recent developments in the modeling of melt pond formation on sea ice (8, 9). To do so, we develop a critical-depth model for regions of the ice-covered Arctic Ocean, incorporating the light-transmitting properties of melt ponds. A recent study [(10), hereafter J16] compared three ice-ocean ecosystem models to evaluate trends in under-ice and Arctic primary production over the past 30 years and found a small overall reduction in sub-ice primary production over this period. However, none of the models contributing to the J16 intercomparison consider melt ponds, which play a role in the development of sub-ice blooms, as discussed below.

On the basis of our modeling study, we find that events like the Chukchi bloom may be routine in the modern Arctic: Over the past decade, the light conditions necessary to permit sub-ice blooms may have existed over nearly 30% of the Arctic region in July. We find these conditions only in the past two decades, driven by a thinning Arctic sea ice cover. The modern Arctic is undergoing a major ecological shift because of climate change: Projections of a thinner Arctic sea ice cover mean that the likelihood and extent of sub-ice phytoplankton blooms may further increase in the future.

## MODEL

The most widely used model for describing the timing and initiation of light-limited phytoplankton blooms is the Sverdrup critical depth hypothesis (11). The critical depth hypothesis has been examined, updated, and expanded in many oceanographic settings (12, 13), although it offers a simplistic treatment of biology and ocean mixing (14, 15). It asserts that phytoplankton populations are continuously mixed vertically within the ocean mixed layer, growing in proportion to the availability of light and dying at a uniform rate. We consider a region of bare sea ice of thickness  $h$ , of which a fraction  $\phi$  is covered by melt ponds, and model the mean specific growth and death rates of a population of phytoplankton in a mixed layer of depth  $D$ . We also assume that ocean velocities are comparable to ice drift velocities, appropriate in the high ice concentration regions considered here, and therefore, as phytoplankton populations grow, they do not advect into regions of different ice cover. Further discussion of this model, which outlines the model equations in

2017 © The Authors,  
some rights reserved;  
exclusive licensee  
American Association  
for the Advancement  
of Science. Distributed  
under a Creative  
Commons Attribution  
NonCommercial  
License 4.0 (CC BY-NC).

<sup>1</sup>Department of Applied Mathematics, School of Engineering and Applied Sciences, Harvard University, Cambridge, MA 02138, USA. <sup>2</sup>Atmospheric, Oceanic and Planetary Physics, Department of Physics, Clarendon Laboratory, University of Oxford, Parks Road, Oxford OX1 3PU, U.K. <sup>3</sup>Department of Earth Sciences, University of Oxford, South Parks Road, Oxford OX1 3AN, U.K. <sup>4</sup>Centre for Polar Observation and Modelling, Department of Meteorology, University of Reading, Reading, U.K.

\*Corresponding author. Email: horvat@fas.harvard.edu

more detail, is provided in Materials and Methods. The mean specific loss rate (per plankton) over the mixed layer is constant

$$L(D) = \Gamma \quad (1)$$

The mean specific growth rate,  $G(D)$ , is proportional to the availability of photosynthetically available radiation (PAR; solar radiation ranging from 400 to 700 nm)

$$G(D) = \frac{\mu I_0}{\kappa_w D} (1 - e^{-\kappa_w D}) [(1 - \alpha_p)\phi + (1 - \alpha_i)(1 - \phi)] e^{-\kappa_i h} \quad (2)$$

Equation 2 is the product of three terms: the first describes the mean growth rate of the phytoplankton population in a region with a mixed layer of depth  $D$  that is ice-free, where  $\kappa_w = 0.12 \text{ m}^{-1}$  (16) is a bulk irradiance extinction coefficient of PAR in clear water, following Beer's law. The coefficient  $\mu$ , which relates the growth rate of phytoplankton to the availability of PAR, is derived from the factor  $\Gamma/\mu$ , termed the "compensation irradiance," which is estimated as  $4.5 \text{ W m}^{-2}$ , based on observations in the North Water Polynya and North Atlantic (see Materials and Methods) (13, 17).  $I_0$  is the PAR incident on the ice or pond surface (in unit  $\text{W m}^{-2}$ ). The second term in Eq. 2 describes the reflection and backscatter of PAR at the ice or pond surface. The disposition of incoming PAR in the ice and to the ocean below is determined by assuming that a shallow scattering layer exists at the ice surface that is included in the parameterization of albedo, where  $\alpha_p = 0.2$  and  $\alpha_i = 0.76$  are the spectral albedos of PAR for melt ponds and bare sea ice, respectively (18–23). The focus of this study is on months in which melt ponds have formed, and therefore, the presence of snow on ice is not a focus here. To avoid unrealistic amounts of solar radiation beneath sea ice in the months before the snow cover melts, we set the ice albedo to that of snow-covered ice,  $\alpha_i = 0.98$  (18, 22, 24), until melt ponds begin to form each year. The third term in Eq. 2 describes how PAR is extinguished within the ice layer. Radiation penetrating the ice is attenuated following Beer's law, with  $\kappa_i = 1.6 \text{ m}^{-1}$ , a bulk irradiance extinction coefficient of PAR in sea ice (19–21). We tested the sensitivity of our results to  $\kappa_i$  (see the Supplementary Materials, text S1, and fig. S1). Although the magnitude of the extent and frequency of sub-ice blooms depends on the choice of  $\kappa_i$ , there are large increasing trends in the extent and frequency of sub-ice blooms across the range of  $\kappa_i$ .

We now seek criteria that determine when a light-limited bloom is permitted. One such criterion occurs when the mixed layer depth shoals above the point where cumulative population growth and decay rates are balanced, at which point the mean specific growth rate exceeds the mean specific death rate and the population grows exponentially. This is a variant of the critical depth hypothesis (11) discussed above, including the effects of a ponded sea ice cover. Nondimensionalizing Eqs. 1 and 2 with  $x \equiv \kappa_w D$ ,  $\beta \equiv \Gamma^{-1} \mu I_0 (1 - \alpha_p) e^{-\kappa_i h}$ , and  $\alpha^* \equiv \frac{1 - \alpha_i}{1 - \alpha_p}$ , this condition occurs when

$$x_c = \beta(1 - e^{-x_c})[\phi + (1 - \phi)\alpha^*] \quad (3)$$

which defines a nondimensional critical depth,  $x_c$ . The original Sverdrup model may be obtained from Eq. 3 by setting  $h = 0$  (when computing  $\beta$ ) and  $\phi = 1$  and replacing the melt pond albedo  $\alpha_p$  with the open-ocean albedo  $\alpha_w = 0.06$ . We can also give a different interpretation of the crit-

ical condition: A bloom occurs when the melt pond fraction increases to permit more light to the ocean below. The critical melt pond fraction  $\phi_c$  is found by rearranging Eq. 3

$$\phi_c = \frac{1}{1 - \alpha^*} \left( \frac{x}{\beta(1 - e^{-x})} - \alpha^* \right) \quad (4)$$

When the melt pond fraction exceeds this critical value, a light-limited bloom is permitted. Therefore, the critical pond hypothesis states that light-limited phytoplankton blooms are triggered annually by a sustained increase in melt pond fraction above  $\phi_c$ .

## RESULTS

### The Chukchi bloom in climatological context

We first examine the likelihood for blooms during a single summer season, using values representative of those observed during the 2011 cruise. Figure 1 (A to D) shows seasonal cycles of the parameters used in the study. Mixed layer depth data are from a combination of observational sources from the Chukchi Sea (Fig. 1A) (25). The ice thickness data used are a representative Arctic Basin seasonal cycle over the period 2000–2012 (Fig. 1B) (26). Solar irradiance data are from the National Centers for Environmental Prediction (NCEP-2) reanalysis climatology at  $72.5^\circ\text{N}$   $170^\circ\text{W}$  (Fig. 1C) (27). An example seasonal cycle of melt pond fraction is taken as the 2012 Arctic-wide mean seasonal cycle from a stand-alone simulation of CICE (Los Alamos sea ice model) (22) that includes a model for the evolution of melt ponds (Fig. 1D) (9, 28). For these values, a light-limited bloom is possible during the period of June to August (green line segments in Fig. 1, A to D), corresponding to the period of maximum solar insolation, maximum melt pond fraction, and minimum mixed layer depth. For many regions of the Arctic with a seasonal ice cover, this may be before the sea ice has melted away. Parameter values observed during the Chukchi bloom are displayed as green circles in Fig. 1 (A to D), with hashed boxes indicating ranges of mixed layer depth (20 to 30 m), ice thickness (0.8 to 1.2 m), and melt pond fraction (30 to 40%) observed during the cruise (7). Crucially, this parameter range permits the formation of a light-limited bloom during the observed period in 2011, beginning as early as mid-June. Therefore, it is possible that the Chukchi bloom may have been diagnosed using the critical depth model outlined here.

We examine the model sensitivity to mixed layer depth by offsetting the reference seasonal cycle of mixed layer depth (Fig. 1A, black line) by  $\pm 8 \text{ m}$  (Fig. 1A, blue dashed and red dash-dot lines). These perturbations are significant relative to the baseline seasonal cycle, which shoals to below 13 m in July, and significantly larger than uncertainty estimates for mixed layer depth in the Chukchi Sea of  $\pm 3.3 \text{ m}$  from a recent mixed layer depth climatology (25). Therefore, this perturbation bounds the sensitivity of this model to uncertainty in mixed layer depth data retrieval and climatology. For each perturbed seasonal cycle, we compute the critical melt pond fraction  $\phi_c$  using Eq. 4 and plot it in Fig. 1E. Each critical melt pond fraction curve corresponds to one of the mixed layer depth curves plotted in Fig. 1A, which is either the reference seasonal cycle (solid black line), a shallower mixed layer (dash-dot red line), or a deeper mixed layer (dashed blue line). The gray line in Fig. 1E is the seasonal cycle of melt pond fraction  $\phi$ , shown in Fig. 1D. When the seasonal melt pond fraction intersects with a critical melt pond fraction curve, the criterion expressed in Eq. 4 is satisfied, and a light-limited bloom is permitted. Phytoplankton populations in shallow mixed layers

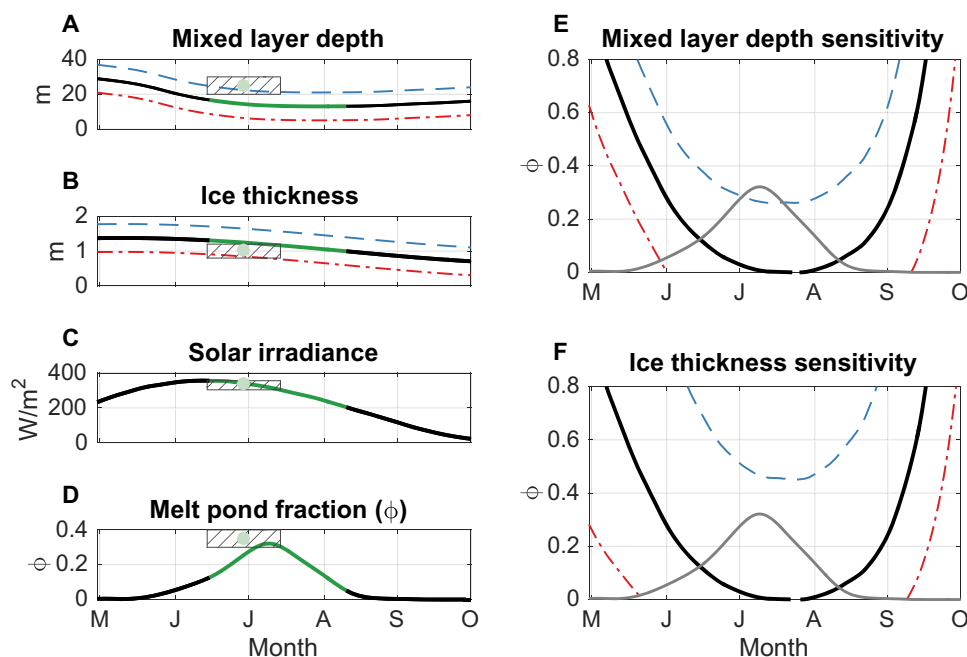


**Fig. 1. Example seasonal cycles of climate variables, timing of sub-ice blooms, and model sensitivity.** (A to D) Example time series of ocean mixed layer depth (A), sea ice thickness (B), surface downwelling solar irradiance (C), and melt pond fraction (D). Blue and red curves in (A) are deviations of  $\pm 8$  m from the reference mixed layer depth curve. Blue and red curves in (B) are deviations in ice thickness of  $\pm 40$  cm from the reference ice thickness curve. Green shaded line segments of the black curves in (A) to (D) indicate a sub-ice bloom is permitted. Green dots and gray boxes correspond to the average observed values and reported ranges observed during the 2011 bloom (4). (E and F) Sensitivity of bloom timing to perturbations in the reference seasonal cycle shown in (A) to (D). (E) The critical melt pond fraction  $\phi_c$  calculated using the seasonal cycles of ocean mixed layer depth displayed in (A) (black solid, red dash-dot, and dashed blue curves). Gray curve is the seasonal cycle of melt pond fraction shown in (D). When curves of  $\phi_c$  are lower than the dashed curves, a light-limited bloom would be permitted in that region. (F) Same as (E) but for the ice thickness seasonal cycles shown in (B).

spend a relatively larger proportion of time in well-illuminated regions, and hence, a reduction in the mixed layer depth leads to an earlier bloom onset, with differences in the timing of a bloom of several weeks. Despite the large offset in the seasonal cycle, blooms are permitted even in the case of the deepest mixed layer.

The timing of sub-ice blooms is strongly sensitive to variations in sea ice thickness. Figure 1F again plots curves of  $\phi_c$ , now corresponding to offsetting the ice thickness seasonal cycle (Fig. 1B, black line) by  $\pm 40$  cm (Fig. 1B, dashed blue and dash-dot red lines). This perturbation is roughly 25% of the reference sea ice thickness in June and is a variation in ice thickness smaller than the observed changes in Arctic sea ice thickness over the past 50 years (29). Therefore, the offset in ice thickness considered in Fig. 1 (B and F) may be considered small relative to the offset examined previously in mixed layer depth (Fig. 1, A and E). Thinner ice attenuates less light and permits blooms as early as mid-May, just as melt ponds begin to form. By contrast, thicker ice attenuates more light and permits no blooms, even when the melt pond fraction is at its maximum. Note that no bloom was observed until 2011 and that the ice in the Chukchi Sea used to be much thicker, a pair of observations that are consistent with our model. This contrasts with the models considered within the J16 intercomparison, which all predict a summer bloom in the Chukchi Sea in every year since 1978. We next consider the issue of Arctic change in more detail.

### Sub-ice blooms in a changing Arctic

Arctic sea ice has changed markedly over the past three decades. The large-scale thinning of sea ice observed in the submarine and satellite record (29) as well as the increase in melt pond fraction seen in satellite observations and model simulations (28, 30) suggest that the potential

for sub-ice blooms has also evolved. We examine a combination of model and reanalysis data over the period 1986–2015 to investigate the potential for a trend of sub-ice phytoplankton blooms in the Arctic.

Daily sea ice thickness, ice concentration, and melt pond fraction are from a stand-alone simulation of the sea ice model CICE (22), including a prognostic model for the evolution of melt ponds (see the Supplementary Materials, text S2, and fig. S2 for maps and time series of these data) (9, 28). The melt pond distributions of the CICE simulation are consistent with in situ observations and pond statistics for the period 2002–2011 based on MODIS satellite data (30–32). Although these existing data are too limited to fully validate the simulated melt pond distribution, the general pattern and evolution of time are within the range of field observations and detailed process studies, which were verified with observations (33, 34).

In recent years, the advent of ice-capable Argo floats (35) that can sample ocean properties in seasonal ice zones, ice-tethered profilers anchored to perennial sea ice (36), and historical hydrographic data bring the possibility of an Arctic mixed layer depth climatology within reach (25). However, data coverage is still neither spatially uniform nor seasonally consistent, and observational gaps exist, particularly in the shallow continental shelves. Therefore, our data on ocean mixed layer depths are taken from the Monthly Isopycnal and Mixed-layer Ocean Climatology (MIMOC), which combines Argo float, ship-board, and ice-tethered profiler data (37). Because of the sparsity of data, we use the same annual cycle of mixed layer depth for each year. As previously discussed, the model is insensitive to perturbations in mixed layer depth. Surface shortwave irradiance data are from the NCEP-2 reanalysis (27). All data are interpolated to a  $0.5^\circ$  by  $0.5^\circ$  grid for latitudes greater than  $60^\circ\text{N}$  and a temporal resolution of 1 per day.



At each ocean grid point, we calculate whether conditions can lead to phytoplankton population growth using the critical pond criterion, Eq. 4. To restrict our interest to only Arctic sub-ice blooms, we excluded grid cells with less than 80% ice concentration, typically defined as the “marginal ice zone,” from the calculation (in contrast to J16, which included these regions when computing under ice primary production). As mentioned above, the marginal ice zone was previously considered the only site where sub-ice phytoplankton blooms were possible (38, 39), but the focus of this study is on blooms underneath sea ice, where open-ocean or marginal ice zone processes, like wind-driven vertical mixing, are less important. We additionally exclude Baffin Bay from the study region to focus on the Arctic Basin alone. The binary data on whether conditions support a bloom are then binned into the calendar months May, June, and July and averaged over each of the time periods 1986–1995, 1996–2005, and 2006–2015. Figure 2 shows the average number of days in each month and each decade that sufficient solar radiation reaches the ocean to satisfy the critical pond hypothesis (because any area with greater than 80% ice concentration at least once during each period is included in the analysis, some regions with an average ice concentration of less than 80% during a given decade are shown as ice-covered in Fig. 2). Estimated sensitivity ranges are provided in the Supplementary Materials and tables S1 and S2.

May sea ice conditions generally do not support sub-ice blooms in all three decades (Fig. 2, A to C), apart from the lower latitudes of the

European Arctic and Kara Sea near the marginal ice zone, where the sea ice is thin. In these locations, sufficient PAR for a phytoplankton bloom penetrates through the ice once per month at most, on average. Conditions leading to a sub-ice bloom are generally not found in the Chukchi Sea at any point in May over any of the analyzed time periods.

The calculated prevalence of sub-ice bloom-permitting conditions during June has increased markedly (Fig. 2, D to F). Over the period 1986–1995, small regions of the European and Russian Arctic near the ice edge and off the coast of Greenland have sufficient light penetration to permit a bloom, up to twice a month on average. From 1996 to 2005, these regions expand, with regions of the European Arctic and Kara Sea having bloom-permitting conditions up to eight times per month (Fig. 2E). In the decade 2006–2015, in the month of June (Fig. 2F), a wide swath of the Russian Arctic has sufficient light conditions to permit a sub-ice bloom at least 5 days per month, with frequencies reaching over 10 days per month in the East Siberian Sea and Kara Sea. Conditions supportive of the massive sub-ice bloom observed in the Chukchi Sea in 2011 (4) are found over the most recent two decades and are much more prevalent from 2006 to 2015. The region in which it was observed (Fig. 2, D to F, red box) experiences a large increase in bloom likelihood over the study period. From 1986 to 1995 (Fig. 2D), the light conditions necessary to support sub-ice blooms occurred with a frequency of less than 1 day per month. Over the period 1996–2005 (Fig. 2E), there was sufficient under-ice light

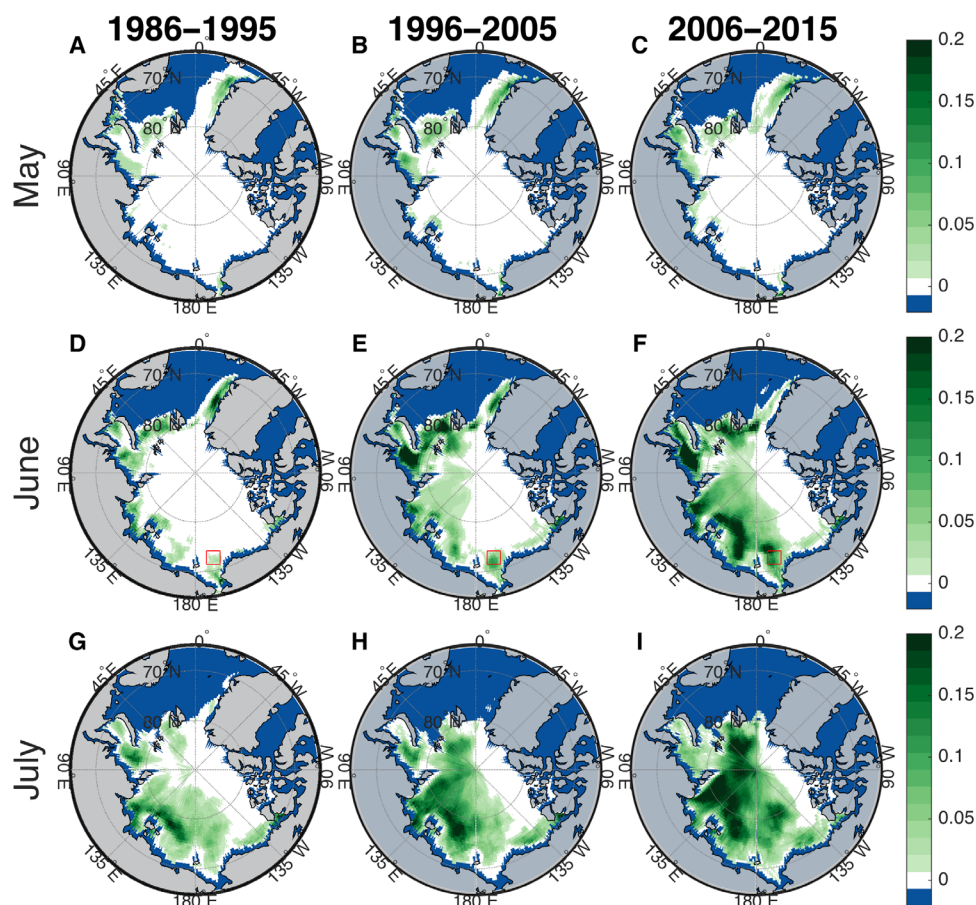


**Fig. 2. Spatial map of the average number of days of sufficient light for sub-ice phytoplankton blooms over time.** (A to C) Shading indicates the number of days in May, from 1986 to 1995 (A), 1996 to 2005 (B), and 2006 to 2015 (C), where a sub-ice bloom is permitted. (D to F) Same as (A) to (C) but for June. (G to I) Same as (A) to (C) but for July. Red boxes in (D) to (F) indicate the region of the 2011 cruise. Baffin Bay and regions with an ice concentration less than 80% at every point during each time period are colored blue. Continents are colored gray.

for a bloom to occur roughly 1 day per month in June. From 2006 to 2015 (Fig. 2F), these conditions arose on average 5 days per month. Light conditions that may lead to the initiation of a sub-ice bloom also occur increasingly throughout the Arctic in July (Fig. 2, G to I), reaching to the interior of the Arctic. From 2006 to 2015, the bloom-permitting conditions arose more than 7 days per month across the Russian and European Arctic and up to 5 days per month in the Chukchi Sea.

To quantify whether a region in the Arctic Ocean (which we again define as all ocean points north of 70°N, excluding Baffin Bay) may have had a sub-ice bloom, a region is defined to be bloom-permitting in each month that it absorbs sufficient light for growth for three consecutive days. Phytoplankton growth rates observed in the 2011 Chukchi bloom exceeded 1 per day; therefore, these bloom-permitting areas permit sufficient light for at least three doublings of the phytoplankton population. Figure 3 (A to C) shows a time series of the fraction of the Arctic Ocean meeting this criterion in each calendar month. The results support the hypothesis that large-scale changes to the sea ice cover have triggered a new ecological paradigm: In June, the fraction of the Arctic supporting sub-ice blooms in each year increases by 5% per decade, from less than 3.0% in 1986 to an average of 13.1% over the period of 2006–2015, with a maximum yearly percentage of 23% in 2007. In July, the effect is similarly significant, increasing by 7% per decade from less than 5% in 1986 to an average of 21.3% over the period 2006–2015, with a maximum of 28% in 2013. Each time series has a significant amount of year-to-year variability in bloom-permitting fraction due to the changing regional ice, ocean, and atmospheric conditions. This level of year-to-year variability in blooming is not demonstrated in the J16 intercomparison.

To attribute these changes to trends in sea ice thickness and melt pond fraction, we perform a set of attribution studies, with results shown in Table 1. In each case, we fix one or more fields (ice concentration  $c$ , melt pond fraction  $\phi$ , or ice thickness  $h$ ) at average values from 1986 to 1995 in each month (May, June, and July). We then compute the percentage of the Arctic that is bloom-permitting from 2006 to 2015, allowing the other variables to vary in time. By comparing the model output when all fields vary together to the output when each trend is suppressed in turn, we can infer which fields have had the most significant limiting effect on the increasing trend demonstrated in Fig. 3. In interpreting the results of Table 1, note that when a field is “fixed,” this removes the effects of the trend in this field (increasing melt pond fraction, decreasing ice thickness, and decreasing total ice concentration).

When the trend in melt pond fraction is suppressed,  $\phi$  is fixed at its mean 1986–1995 values, and sea ice thickness and concentration vary.

In this case, 7.9% of the Arctic Ocean permits blooms in June and 16.2% in July over 2006–2015. When the trend in sea ice thickness is suppressed instead and  $\phi$  varies in time, the fraction of the Arctic Ocean that supports sub-ice blooms over 2006–2015 is 1.5% in June and 2.2% in July. From this, we infer that the thinning of sea ice has had a more significant direct effect on the increasing spatial coverage of bloom-permitting regions in June and July than has the increasing trend in melt pond fraction.

Over the period 1986–2015, the area covered by sea ice in the Arctic has decreased significantly (see the Supplementary Materials and fig S2). The percentages reported above are computed as fractions of the Arctic Ocean, not of the ice-covered regions. Any increase in bloom-permitting fraction occurs despite the declining ice-covered area, which has reduced the available percentage of the Arctic Ocean that could permit sub-ice blooms from May to July. We can evaluate the significance of the declining sea ice area coverage by fixing the sea ice concentration field at its 1986–1995 average values. In this case, the fraction of the Arctic that has sufficient light to permit sub-ice blooms is 2.1% in May, 16.0% in June, and 31.1% in July on average over the period 2006–2015, indicating that the decrease in sea ice area coverage has decreased the extent of the Arctic that may experience sub-ice blooms. Regions that were ice-covered from 1986 to 1995, but not from 2006 to 2015, may still experience phytoplankton blooms tied to the retreating ice edge, as discussed in the study of Perrette *et al.* (3).

To consider whether trends in bloom-permitting fraction may be suppressed by the declining sea ice area over the period 1986–2015, we consider the bloom-permitting fraction over 2006–2015 when the ice concentration field is fixed at its 1986–1995 average. When the ice thickness trend is also held at its 1986–1995 average, a smaller proportion of the Arctic is found to be bloom-permitting than when the melt pond fraction is also held at its 1986–1995 average (1.1% versus 11.6% in June and 2.0% versus 29.5% in July).

Both Pan-Arctic average sea ice thickness and melt pond fraction have significant trends over the study period (see the Supplementary Materials and fig S2). From these attribution studies, we conclude that the direct cause of the increase in Pan-Arctic bloom potential is a declining sea ice thickness field, with the increasing trend in melt pond fraction having a comparatively insignificant effect. This does not account for the relationship between pond fraction and sea ice thickness. Melt ponds are significant for sub-ice blooms in two ways. First, sea ice thinning is enhanced by increasing melt pond fraction. Because of the reduced surface albedo of ponded ice, melt ponds increase the absorption

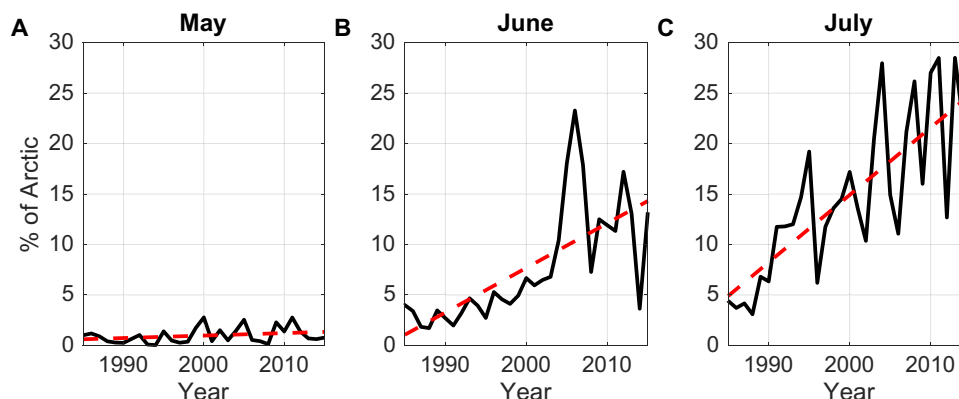


**Fig. 3. Evolution and variability of the pan-Arctic likelihood of sub-ice blooms over time.** (A to C) Percentage by area of the Arctic Ocean that has greater than 80% ice concentration and permits growth for at least three consecutive days in May (A), June (B), and July (C). Red dashed lines are linear fits to the data.

**Table 1. Analysis of the causes of changes in sub-ice blooms in the Arctic Ocean.** The average fraction of the Arctic Ocean that permits a light-limited sub-ice bloom from 2006 to 2015 when labeled external fields are held constant at their mean 1986–1995 values. The Arctic is defined as the region with latitudes greater than 70°N, excluding Baffin Bay. Percentage by area refers to the average area of the Arctic with an ice concentration greater than 80%, in which at least three consecutive days permit enough light for a light-limited bloom to occur, averaged over the time period 2006–2015. The notation “x fixed” refers to output when the variable *x* is fixed at its mean 1986–1995 values. Variables that may be fixed are the ice thickness *h*, melt pond fraction  $\phi$ , and ice concentration *c*. The final row is the average fraction of the Arctic Ocean that permits a light-limited sub-ice bloom from 2006 to 2015 when the melt pond fraction  $\phi$  is always equal to zero.

	May % area	June % area	July % area
None fixed	1.1%	13.1%	21.4%
<i>h</i> fixed	0.3%	1.5%	2.2%
$\phi$ fixed	3.5%	7.9%	16.2%
<i>c</i> fixed	2.1%	16.0 %	31.1%
<i>h</i> , <i>c</i> fixed	0.3%	1.1%	2.0%
$\phi$ , <i>c</i> fixed	5.5%	11.6%	29.5%
$\phi$ , <i>h</i> fixed	0.9%	1.4 %	1.6%
$\phi = 0$	0.8%	4.4%	6.1%

of solar radiation within the sea ice itself, thereby boosting its melting and thinning it (20, 21). CICE simulations that include the prognostic evolution of melt ponds have thinner ice than those that do not (9). Over the period 2006–2015, ice thickness is reduced in simulations with melt pond evolution by 3.8 cm in May, 4.5 cm in June, and 25.2 cm in July in the ice-covered regions considered by our analysis. Second, melt ponds are needed for there to be a significant overall potential for sub-ice blooming. When the melt pond fraction is set to be zero in all ice-covered regions, the percentage of the Arctic that is bloom-permitting from 2006 to 2015 is less than 1% in May, 4.4% in June, and 6.1% in July (Table 1, final row).

## DISCUSSION

The observation of a phytoplankton bloom underneath sea ice in July 2011 represented a major change in the scientific understanding of the Arctic Ocean and its ecology. We find that this may be a consequence of the thinning of the Arctic sea ice cover observed over the satellite era. Sea ice conditions permitting sufficient PAR for sub-ice blooms have become common in the present-day Arctic, having been rare 30 years ago. In our analysis, we find that these conditions may have existed over 30% of the Arctic in recent years, in the months of June and July, with changes driven primarily by declining sea ice thickness. This indicates that climate change has markedly altered the ecological underpinnings of the Arctic Ocean and its carbon cycle (40). The greater-than-expected net primary productivity under sea ice has been discussed in the context of the Chukchi bloom (4, 7). Therefore, those authors' extrapolations of the impacts of these blooms on the Arctic carbon cycle based on the Chukchi bloom are supported by our modeling study.

The model described above is based on the long-standing paradigm that blooms in the Arctic Ocean are light-limited, as evidenced by the

fact that they are tied to the seasonal retreat of the ice edge (3). This is only a necessary condition for sub-ice blooms. The presence or lack of nutrients may also limit the genesis of blooms. Therefore, predictions of sub-ice blooms in the modern Arctic will require modeling of the under-ice nutrient distribution alongside the light distribution to support and confirm contemporaneous observations. Observing these blooms remains a challenge because satellites do not observe chlorophyll through sea ice and ship-based measurements are expensive and localized. Therefore, the results of this study should prove useful for planning future expeditions aimed at observing these blooms. We would suggest the use of moorings in the high-bloom likelihood regions seen in Fig. 2, in the Chukchi Sea or Russian Arctic, to validate the results presented above and observe the Pan-Arctic frequency of sub-ice blooms. In the future, because the Arctic sea ice continues to thin, the frequency and extent of June and July blooms may increase even further. The specific consequences of this marked shift in the Arctic marine ecosystem and carbon budget are an important area for future inquiry.

## MATERIALS AND METHODS

### Sub-ice critical depth model

The time evolution of the cumulative population of phytoplankton  $\mathcal{P}(D)$ , over a mixed layer of depth *D*, is described by the equation

$$\frac{\partial \mathcal{P}(D)}{\partial t} = (G(D) - L(D))\mathcal{P}(D) \quad (5)$$

where  $G(D)$  (in unit  $s^{-1}$ ) is the mean specific (per plankter) growth rate up to a depth *D* and  $L(D)$  (in unit  $s^{-1}$ ) is similarly the mean specific population loss rate up to a depth *D*. Equation 5 implies that the phytoplankton population grows exponentially when growth exceeds loss [ $G(D) - L(D) > 0$ ].

The mean growth rate  $G(D)$  of phytoplankton populations depends on converting solar radiation ranging from 400 to 700 nm, known as PAR, into energy. In a region covered by sea ice of thickness *h*, we modeled the PAR at a depth *z* below the ice according to previous studies (18, 19)

$$I_i(z) = I_0(1 - a_i)e^{-\kappa_i h}e^{\kappa_w z}$$

where  $I_0$  is the PAR incident on the ice surface (in unit  $W m^{-2}$ ),  $\alpha_i = 0.76$  is the albedo of bare ice assuming a shallow scattering layer at the ice surface,  $\kappa_w = 0.12 m^{-1}$  is the coefficient of extinction of PAR in clear water,  $\kappa_i \approx 1.6$  (in unit  $m^{-1}$ ) is the extinction coefficient of PAR in sea ice, both following Beer's law, and *z* is negative downward. Pondered ice has a surface albedo  $\alpha_p = 0.2$  that accounts for scattering within the pond layer; therefore, the radiation penetrating the pond to the ice below is  $(1 - \alpha_p)I_0$ . The PAR,  $I_m(z)$ , under a melt pond at a depth *z* for ice of thickness *h* is

$$I_m(z) = I_0 e^{(-\kappa_i h)} (1 - \alpha_p) e^{\kappa_w z}$$

We assumed that phytoplankton populations are well mixed laterally on scales larger than the typical spacing of melt ponds and respond to a weighted average of the PAR by melt pond area fraction. The total



PAR,  $I(z)$ , underneath a region of ponded ice of thickness  $h$  and melt pond area fraction  $\phi$  is

$$I(z) = \phi I_m(z) + (1 - \phi) I_i(z), \\ = I_0 e^{-\kappa_i h} [(1 - a_p)\phi + (1 - \phi)(1 - a_i)] e^{-\kappa_w z} \quad (6)$$

Phytoplankton growth at depth  $z$  was assumed to be linearly related to the light intensity  $I(z)$  with a proportionality coefficient  $\mu$  (in unit  $\text{m} \Gamma^{-1}$ ) (11). Phytoplankton decay was assumed uniform, independent of  $z$ , at a rate  $\Gamma$  (in unit  $\text{m}^{-1} \text{s}^{-1}$ ). The mean growth rate was then determined by integrating Eq. 6

$$G(D) = \frac{\mu}{D} \int_{-D}^0 I(z) dz \\ = \frac{\mu I_0}{\kappa_w D} (1 - e^{-\kappa_w D}) \times [(1 - a_p)\phi + (1 - \phi)(1 - a_i)] \times e^{-\kappa_i h}$$

The mean death rate  $L(D)$  is simply

$$L(D) = \frac{1}{D} \int_{-D}^0 \Gamma dz = \Gamma$$

### Parameters used to evaluate sub-ice blooms

The compensation irradiance,  $\Gamma/\mu$  was estimated using data from the North Water Polynya (17), with units of  $\text{mol quanta m}^{-2} \text{d}^{-1}$  (where  $\text{d} = \text{day}$ ) and a range of  $1.9 \pm 0.3 \text{ mol quanta m}^{-2} \text{d}^{-1}$ .  $\Gamma/\mu$  was measured in the North Atlantic via satellite (13), with values in a similar range ( $1.3 \pm 0.3$ ), although to the authors' knowledge, no similar measurements exist in the high Arctic. On the basis of this similarity, we assumed that the magnitude of this factor is relatively spatially uniform and in this range in the Arctic. The conversion factor from these units to  $\text{W m}^{-2}$  was approximately  $2.5 \text{ W mol}^{-1} \text{ quanta d}^{-1}$  for PAR from sunlight; thus, we approximated  $\Gamma/\mu = 4.5 \text{ W m}^{-2}$  as a representative value. The clear-water attenuation coefficient ranged from 0.09 to  $0.16 \text{ m}^{-1}$  for wavelengths in the range (412,555) (16). We chose  $0.12 \text{ m}^{-1}$  as a representative value.

### SUPPLEMENTARY MATERIALS

Supplementary material for this article is available at <http://advances.sciencemag.org/cgi/content/full/3/3/e1601191/DC1>

text S1. Sensitivity to extinction coefficient in ice.

text S2. Evolution of fields over time.

text S3. Sensitivity analysis: Bounds on the area that permits sub-ice blooms.

fig. S1. Sensitivity of bloom-permitting area to ice extinction coefficient.

fig. S2. Evolution of ice concentration, melt pond fraction, and ice thickness over time.

table S1. Ranges of the percentage of the Arctic Ocean ( $>70^\circ\text{N}$ , excluding Baffin Bay) in which sub-ice blooms can occur, when sea ice thickness data are increased or decreased by 1 SD (for details on how this is computed, see text S2).

table S2. Ranges of the percentage of the Arctic Ocean ( $>70^\circ\text{N}$ , excluding Baffin Bay) in which sub-ice blooms can occur, when the melt pond coverage data are increased or decreased by 1 SD (for details on how this is computed, see text S2).

### REFERENCES AND NOTES

- C. L. Sabine, R. A. Feely, N. Gruber, R. M. Key, K. Lee, J. L. Bullister, R. Wanninkhof, C. S. Wong, D. W. R. Wallace, B. Tilbrook, F. J. Millero, T.-H. Peng, A. Kozyr, T. Ono, A. F. Rios, The oceanic sink for anthropogenic  $\text{CO}_2$ . *Science* **305**, 367–371 (2004).
- M. J. Behrenfeld, E. S. Boss, Resurrecting the ecological underpinnings of ocean plankton blooms. *Ann. Rev. Mar. Sci.* **6**, 167–194 (2014).
- M. Perrette, A. Yool, G. D. Quartly, E. E. Popova, Near-ubiquity of ice-edge blooms in the Arctic. *Biogeosciences* **8**, 515–524 (2011).
- K. R. Arrigo, D. K. Perovich, R. S. Pickart, Z. W. Brown, G. L. van Dijken, K. E. Lowry, M. M. Mills, M. A. Palmer, W. M. Balch, F. Bahr, N. R. Bates, C. Benitez-Nelson, B. Bowler, E. Brownlee, J. K. Ehn, K. E. Frey, R. Garley, S. R. Laney, L. Lubelczyk, J. Mathis, A. Matsuoka, B. G. Mitchell, G. W. K. Moore, E. Ortega-Retuerta, S. Pal, C. M. Polashenski, R. A. Reynolds, B. Schieber, H. M. Sosik, M. Stephens, J. H. Swift, Massive phytoplankton blooms under Arctic sea ice. *Science* **336**, 1408 (2012).
- M. A. Palmer, B. T. Saenz, K. R. Arrigo, Impacts of sea ice retreat, thinning, and melt-pond proliferation on the summer phytoplankton bloom in the Chukchi Sea, Arctic Ocean. *Deep Sea Res. Part II* **105**, 85–104 (2014).
- C. J. Mundy, M. Gosselin, J. Ehn, Y. Gratton, A. Rossnagel, D. G. Barber, J. Martin, J.-. Tremblay, M. Palmer, K. R. Arrigo, G. Darnis, L. Fortier, B. Else, T. Papakyriakou, Contribution of under-ice primary production to an ice-edge upwelling phytoplankton bloom in the Canadian Beaufort Sea. *Geophys. Res. Lett.* **36**, L17601 (2009).
- K. R. Arrigo, D. K. Perovich, R. S. Pickart, Z. W. Brown, G. L. van Dijken, K. E. Lowry, M. M. Mills, M. A. Palmer, W. M. Balch, N. R. Bates, C. R. Benitez-Nelson, E. Brownlee, K. E. Frey, S. R. Laney, J. Mathis, A. Matsuoka, B. G. Mitchell, G. W. K. Moore, R. A. Reynolds, H. M. Sosik, J. H. Swift, Phytoplankton blooms beneath the sea ice in the Chukchi sea. *Deep Sea Res. Part II* **105**, 1–16 (2014).
- D. Flocco, D. L. Feltham, A. K. Turner, Incorporation of a physically based melt pond scheme into the sea ice component of a climate model. *J. Geophys. Res. Oceans* **115**, C08012 (2010).
- D. Flocco, D. Schroeder, D. L. Feltham, E. C. Hunke, Impact of melt ponds on Arctic sea ice simulations from 1990 to 2007. *J. Geophys. Res. Oceans* **117**, C09032 (2012).
- M. Jin, E. E. Popova, J. Zhang, R. Ji, D. Pendleton, Ø. Varpe, A. Yool, Y. J. Lee, Ecosystem model intercomparison of under-ice and total primary production in the Arctic Ocean. *J. Geophys. Res. Oceans* **121**, 934–948 (2016).
- H. U. Sverdrup, On conditions for the vernal blooming of phytoplankton. *J. Cons. Perm. Int. Explor. Mer.* **18**, 287–295 (1953).
- V. Smetacek, U. Passow, Spring bloom initiation and Sverdrup's critical-depth model. *Limnol. Oceanogr.* **35**, 228–234 (1990).
- D. A. Siegel, S. C. Doney, J. A. Yoder, The North Atlantic spring phytoplankton bloom and Sverdrup's critical depth hypothesis. *Science* **296**, 730–733 (2002).
- M. J. Behrenfeld, Abandoning Sverdrup's critical depth hypothesis on phytoplankton blooms. *Ecology* **91**, 977–989 (2010).
- J. R. Taylor, R. Ferrari, Shutdown of turbulent convection as a new criterion for the onset of spring phytoplankton blooms. *Limnol. Oceanogr.* **56**, 2293–2307 (2011).
- W. S. Pegau, Inherent optical properties of the central Arctic surface waters. *J. Geophys. Res.* **107**, SHE 16–1–SHE 16–7 (2002).
- J.-É. Tremblay, C. Michel, K. A. Hobson, M. Gosselin, N. M. Price, Bloom dynamics in early opening waters of the Arctic Ocean. *Limnol. Oceanogr.* **51**, 900–912 (2006).
- E. E. Ebert, J. A. Curry, An intermediate one-dimensional thermodynamic sea ice model for investigating ice-atmosphere interactions. *J. Geophys. Res.* **98**, 10085–10109 (1993).
- E. E. Ebert, J. L. Schramm, J. A. Curry, Disposition of solar radiation in sea ice and the upper ocean. *J. Geophys. Res.* **100**, 15965–15975 (1995).
- B. Light, T. C. Grenfell, D. K. Perovich, Transmission and absorption of solar radiation by Arctic sea ice during the melt season. *J. Geophys. Res.* **113**, C03023 (2008).
- B. Light, D. K. Perovich, M. A. Webster, C. Polashenski, R. Dadić, Optical properties of melting first-year Arctic sea ice. *J. Geophys. Res. Oceans* **120**, 7657–7675 (2015).
- E. C. Hunke, W. H. Lipscomb, A. K. Turner, N. Jeffery, S. Elliott, "CICE: The Los Alamos sea ice model documentation and software user's manual version 5.1" (Technical Report No. LA-CC-06-012, Los Alamos National Laboratory, 2015).
- L. Istomina, G. Heygster, M. Huntemann, P. Schwarz, G. Birnbaum, R. Scharien, C. Polashenski, D. Perovich, E. Zege, A. Malinka, A. Prikhach, I. Katsev, Melt pond fraction and spectral sea ice albedo retrieval from MERIS data—Part 1: Validation against in situ, aerial, and ship cruise data. *Cryosphere* **9**, 1551–1566 (2015).
- T. C. Grenfell, G. A. Maykut, The optical properties of ice and snow in the Arctic Basin. *J. Glaciol.* **18**, 445–463 (1977).
- C. Peralta-Ferriz, R. A. Woodgate, Seasonal and interannual variability of pan-Arctic surface mixed layer properties from 1979 to 2012 from hydrographic data, and the dominance of stratification for multiyear mixed layer depth shoaling. *Prog. Oceanogr.* **134**, 19–53 (2015).
- R. Lindsay, A. Schweiger, Arctic sea ice thickness loss determined using subsurface, aircraft, and satellite observations. *Cryosphere* **9**, 269–283 (2015).
- M. Kanamitsu, W. Ebisuzaki, J. Woollen, S.-K. Yang, J. J. Niilo, M. Fiorino, G. L. Potter, NCEP–DOE AMIP-II reanalysis (R-2). *Bull. Am. Meteorol. Soc.* **83**, 1631–1643 (2002).
- D. Schröder, D. L. Feltham, D. Flocco, M. Tsamados, September Arctic sea-ice minimum predicted by spring melt-pond fraction. *Nat. Clim. Change* **4**, 353–357 (2014).
- R. Kwok, D. A. Rothrock, Decline in Arctic sea ice thickness from submarine and ICESat records: 1958–2008. *Geophys. Res. Lett.* **36**, L15501 (2009).

30. A. Rösel, L. Kaleschke, Exceptional melt pond occurrence in the years 2007 and 2011 on the Arctic sea ice revealed from MODIS satellite data. *J. Geophys. Res. Oceans* **117**, C05018 (2012).
31. F. Fetterer, N. Untersteiner, Observations of melt ponds on Arctic sea ice. *J. Geophys. Res. Oceans* **103**, 24821–24835 (1998).
32. H. Eicken, T. C. Grenfell, D. K. Perovich, J. A. Richter-Menge, K. Frey, Hydraulic controls of summer Arctic pack ice albedo. *J. Geophys. Res. Oceans* **109**, C08007 (2004).
33. M. Lũthje, D. L. Feltham, P. D. Taylor, M. G. Worster, Modeling the summertime evolution of sea-ice melt ponds. *J. Geophys. Res.* **111**, C02001 (2006).
34. F. Scott, D. L. Feltham, A model of the three-dimensional evolution of Arctic melt ponds on first-year and multiyear sea ice. *J. Geophys. Res.* **115**, C12064 (2010).
35. O. Klatt, O. Boebel, E. Fahrbach, A profiling float's sense of ice. *J. Atmos. Oceanic Tech.* **24**, 1301–1308 (2007).
36. J. M. Toole, M.-L. Timmermans, D. K. Perovich, R. A. Krishfield, A. Proshutinsky, J. A. Richter-Menge, Influences of the ocean surface mixed layer and thermohaline stratification on Arctic Sea ice in the central Canada Basin. *J. Geophys. Res.* **115**, C10018 (2010).
37. S. Schmidtko, G. C. Johnson, J. M. Lyman, MIMOC: A global monthly isopycnal upper-ocean climatology with mixed layers. *J. Geophys. Res. Oceans* **118**, 1658–1672 (2013).
38. K. R. Arrigo, G. L. van Dijken, Phytoplankton dynamics within 37 Antarctic coastal polynya systems. *J. Geophys. Res.* **108**, 3271 (2003).
39. Y. Li, R. Ji, S. Jenouvrier, M. Jin, J. Stroeve, Synchronicity between ice retreat and phytoplankton bloom in circum-Antarctic polynyas. *Geophys. Res. Lett.* **43**, 2086–2093 (2016).
40. A. D. McGuire, L. G. Anderson, T. R. Christensen, S. Dallimore, L. Guo, D. J. Hayes, M. Heimann, T. D. Lorenson, R. W. Macdonald, N. Roulet, Sensitivity of the carbon cycle in the Arctic to climate change. *Ecol. Monogr.* **74**, 523–555 (2009).

**Acknowledgments:** We thank A. Wells and M. Miller for their most helpful comments on an earlier version of this manuscript. C.H., S.I., D.R.J., and D. Flocco attended a Mathematical Research Community supported by this grant on “Differential Equations, Probability, and Sea Ice,” and acknowledge helpful and illuminating discussions with many of the participants, particularly K. Golden and C. Barry. **Funding:** This work was supported by the NSF under grant no. 1321794. D.R.J. acknowledges support from the John Fell Oxford University Press Research Fund. C.H. was supported by the Department of Defense through the National Defense Science and Engineering Graduate Fellowship Program. **Author contributions:** C.H. conceived the model. C.H., S.I., and D.R.J. developed the model equations, performed the analysis of the model equations, and jointly wrote and edited the manuscript. D. Flocco also discussed the model development at the outset of the project. C.H., S.I., D.R.J., and D.S. subsequently designed the Arctic change and sensitivity analyses, which C.H. performed. D.S., D. Flocco, and D. Feltham provided model data and analysis for the Arctic change section. All authors jointly discussed and analyzed the data, results, conclusions, and implications. **Competing interests:** The authors declare that they have no competing interests. **Data and materials availability:** All data needed to evaluate the conclusions in the paper are present in the paper and/or the Supplementary Materials. Additional data related to this paper may be requested from the authors.

Submitted 26 May 2016

Accepted 10 February 2017

Published 29 March 2017

10.1126/sciadv.1601191

**Citation:** C. Horvat, D. R. Jones, S. Iams, D. Schroeder, D. Flocco, D. Feltham, The frequency and extent of sub-ice phytoplankton blooms in the Arctic Ocean. *Sci. Adv.* **3**, e1601191 (2017).



This article is published under a Creative Commons license. The specific license under which this article is published is noted on the first page.

For articles published under [CC BY](#) licenses, you may freely distribute, adapt, or reuse the article, including for commercial purposes, provided you give proper attribution.

For articles published under [CC BY-NC](#) licenses, you may distribute, adapt, or reuse the article for non-commercial purposes. Commercial use requires prior permission from the American Association for the Advancement of Science (AAAS). You may request permission by clicking [here](#).

***The following resources related to this article are available online at <http://advances.sciencemag.org>. (This information is current as of April 19, 2017):***

**Updated information and services**, including high-resolution figures, can be found in the online version of this article at:  
<http://advances.sciencemag.org/content/3/3/e1601191.full>

**Supporting Online Material** can be found at:  
<http://advances.sciencemag.org/content/suppl/2017/03/27/3.3.e1601191.DC1>

This article **cites 39 articles**, 3 of which you can access for free at:  
<http://advances.sciencemag.org/content/3/3/e1601191#BIBL>

*Science Advances* (ISSN 2375-2548) publishes new articles weekly. The journal is published by the American Association for the Advancement of Science (AAAS), 1200 New York Avenue NW, Washington, DC 20005. Copyright is held by the Authors unless stated otherwise. AAAS is the exclusive licensee. The title *Science Advances* is a registered trademark of AAAS